Epistasis supports viability under extensive gene-dose insufficiency following chromosome loss

Hanna Tutaj, Katarzyna Tomala, Ryszard Korona

Institute of Environmental Sciences, Jagiellonian University, Cracow, Poland

Corresponding author:
Ryszard Korona; +048 510 071 693; ryszard.korona@uj.edu.pl

Abstract

Chromosome loss results in halving the dose of multiple genes. We reasoned that yeast monosomic strains would constitute a relatively simple model suited to address the complex question of how extant diploid organisms can stay relatively fit despite harboring numerous function-canceling (mostly heterozygous) mutations. We started by re-examining diploid yeast strains with a single heterozygous gene deletion and ascertained that many of them produced small but measurable growth defects. Mapped to individual chromosomes, they often combined into burdens sufficient to turn the growth rate negative, that is, inflict lethality. However, the subsequently derived monosomics did experience such loads yet continued to proliferate as if much (often most) of the harm introduced by single mutations disappeared. This constitutes an outstanding example of positive epistasis for fitness. We then sought its functional explanation by analyzing transcriptomes. There was no evidence for widespread gene-dose compensation or cellular stress response. Alterations were abundant but not parallel. A notable exception was the general upregulation of genes coding for ribosomal proteins and the concomitant downregulation of those coding for the proteasome. It indicates that the (irreparably) distorted stoichiometry of ribosomal proteins was the most common and critical impediment to growth and eclipsed the impact of other metabolic insufficiencies. In general terms, the modular structure of the cell leads to effective fragmentation of the total burden of mutations. Those located outside the module(s) currently defining fitness lose at least some of their relevance which produces the epiphenomenon of positive epistasis between individually negative effects.

Introduction

A typical human germline cell has as many as one hundred inactive genes, usually complemented by active alleles (MacArthur et al., 2012). Somatic cell lines in healthy tissues add dozens of new (nearly always heterozygous) mutations every year (Moore et al., 2021). Understanding how this burden of DNA damage translates into the mutational load, defined as a decrease in fitness, has proved to be demanding, not only in the case of humans but also simpler organisms. Estimates of selection and dominance coefficients of single mutations tend to be imprecise, any quantification of interactions between multiple mutations (epistasis) appears even more challenging (Henn et al., 2015). The difficulty with the gene interactions is not just technical but primarily methodological. Any comprehensive research on epistasis would require that the studied combinations of mutations represented an unbiased sample of all possible. The actual combinations encountered in the extant organisms (cells) do not satisfy this requirement because they represent samples distorted by natural selection. For example, the discovery that the individuals whose fitness is negatively impacted by epistasis are underrepresented or even absent cannot be unequivocally interpreted. Either the negative interactions are originally rare or organisms affected by them are eliminated before being scored. Similarly, the presence of multiple and undoubtedly deleterious mutations in an otherwise well-performing organism may mean that either their negative effects tend to alleviate each other or that some yet-unrecognized genetic compensations have developed.

As the fitness architecture of naturally occurring organisms is difficult to disentangle, researchers turned to simpler systems. In the model organism of *Saccharomyces cerevisiae,* collections of engineered single-gene mutations, such as complete deletions, have been created and used to estimate the selection and dominance coefficients as well as the effects of interaction between a few (typically two) loci (Costanzo et al., 2010; Giaever et al., 2002; Steinmetz et al., 2002). It would be much more difficult to combine large numbers of harmful mutations. This unavoidably long process would expose the strains under construction to a high probability of developing fitness-restoring genetic adjustments which are known to arise even under limited propagation (Szamecz et al., 2014). A rapid way to generate genomes with extensive loads of known mutations is needed. With this in mind, we noted that the budding yeast genome is composed of roughly five thousand genes that are split among 16 chromosomes in a mostly random fashion. We reasoned that monosomy, the loss of one chromosome in an otherwise regular diploid, $2n$-1, would mean sudden mutation (partial inactivation) of numerous and arbitrarily assembled genes.

Results

<u>Viability of monosomic strains</u>

We began our study by inserting three markers into one chromosome within each homologous pair. These were two *URA3* genes, each at the center of every arm, and one copy of *kan* close to a centromere (Tutaj et al., 2022). As its homolog was unmarked, mutants lacking the markers signaled a possible loss of the marked chromosome (Materials and Methods). We expected that

such generated genuine monosomic strains (M1, M2, …, M16) would exhibit visible growth defects which we indeed observed, except for M1 (**Fig. 1a**). The loss of markers and slow growth were only hints and proved false on several occasions when sequencing of DNA revealed that the expected loss of a single chromosome did not happen, or it did but was accompanied by other changes. **Fig. 1b** presents isolates that passed the sequencing test. As **Fig. 1c** shows, small colonies formed by monosomic cells were regularly infested by much bigger ones. For every monosomic, at least dozens of the latter were re-streaked and found to reproduce the fast-growth phenotype nearly universally. To prevent them from overgrowing the monosomics, we had to keep the cultures small, down to 5 µl of the YPD medium in the case of M5 or M15. The cultures had to be highly replicated so that a sufficient number of those dominated by the slow-growing cells could be still found and recurrently replenished.

The described above procedure could not be completed for three chromosomes—VII, XII, and XIII—even though we paid especially much attention to them. Regarding screens for M7 and M13, we did not find a single mutant that lacked the markers, grew slowly and could rapidly revert to a normal phenotype. Instead, we regularly encountered isolates of the searched genotype without a growth defect and with a diploid genome. Hypothetically, two mitotic cross-overs within a pair of homologous chromosomes could produce one progeny cell without the markers. We were able to reject this possibility based on the results of the present study and a former one (Tutaj et al., 2022). Relevant data and calculations are provided in **Supplementary Text**. The only viable explanation is that the marked chromosomes VII and XIII had been lost and their non-marked homologs underwent endoreduplication shortly after that. Thus, M7 and M13 were probably not inviable but prohibitively unstable. (They could suffer from very slow growth, a high rate of endoreduplication, or both.) Searching for M12, we obtained unusually numerous and genotypically variable isolates but none correct in terms of growth phenotype or DNA copy number mapping (Materials and Methods, **Supplementary Text**). Chromosome XII contains the only yeast rDNA region and is a strong recombinational hotspot (Tutaj et al., 2022). Therefore, we suspended attempts to derive M12, especially since, as we show below, its predicted burden of haploinsufficiency was well within the range covered by other chromosomes.

We sought to include all monosomic in our assays in order to test whether monosomy can occur and persist in absence of other genetic changes. In the wild, monosomic isolates have been found only for a few and the shortest chromosomes (Peter et al., 2018). Similar scope of monosomy has been detected in mutation-accumulation experiments (Sui et al., 2020; Zhu et al., 2014). It is unsure whether these monosomies were simply tolerated, compensated by other changes, or conditionally adaptive, especially in natural environments. There have been laboratory experiments signaling that all monosomies can be induced in yeast but this likely happened only transiently as these studies relied on screening for the loss of heterozygosity at selected loci only (Beach et al., 2017; Reid et al., 2008). Thus, former work on yeast monosomy should be taken cautiously and the future one planned properly. Colonies of presumed monosomics can be actually diploids of complex aneuploids. Those initially truly monosomic are

117 readily overtaken by endo-reduplications or other compensations of the chromosome loss (within
118 even a moderately sized colony). Here we combined the marker-based approach with genome-
119 wide tests based on sequencing DNA (reported above) and RNA (below) to confirm that pure,
120 genetically non-compensated, yeast monosomics are viable.
121
122 Epistasis for fitness
123 Before studying epistasis among multiple mutations, their single effects should be known
124 sufficiently well. Regarding the yeast growth rate, effectively none of single gene deletions can
125 make it faster (Sliwa and Korona, 2005). About 1/5 of them stop growth altogether and another
126 1/5 decelerate it detectably (Giaever et al., 2002). These estimates refer to homozygous or
127 haploid strains under optimal laboratory conditions. Heterozygous deletions, again under good
128 conditions, exhibit morphological alterations quite often but their growth rate, i.e., proliferative
129 fitness, is affected rarely and only modestly (Deutschbauer et al., 2005; Marek and Korona,
130 2016; Ohnuki and Ohya, 2018). In Materials and Methods, we explain how we selected 468
131 heterozygous single deletion strains as those likely (haplo)insufficient for growth on rich
132 medium, YPD. We applied replicated growth rate measurements for individual deletion strains
133 and compared them to a set of carefully selected control strains in order to make our estimates
134 possibly precise and reliable. Doubling rates of individual heterozygous deletions were divided
135 by that of the control to yield relative doubling rates, *rDR*s (**Datasheet 1**) The frequency
136 distribution of *rDR* is shown in **Fig. 2a**. It demonstrates that the negative effects of deletions
137 were undoubtedly present although predictably small, a sizable fraction of them was on the order
138 of the bidirectional effects of the phenotypic plasticity and/or measurement errors (as exposed by
139 the variation within genetically homogeneous control).
140 Epistasis is absent when an effect of a gene variant does not depend on the genetic
141 content of other loci. In the case of fitness, a non-neutral mutation corresponds to a proportional
142 change of wild-type fitness (Crow and Kimura, 1971). An absence of epistasis means that the
143 fitness quotient of a particular mutation remains unchanged irrespective of whether it is the only
144 one present in an individual or accompanied by other fitness-affecting mutations. Accepting this
145 postulate is equivalent to adopting a multiplicative model of fitness structure under which the
146 fitness of a genotype involving n loci is the product of n respective quotients. The model is
147 additive for log-fitness because such a transformation turns a quotient into a deviation from one
148 and a product of quotients into a sum of such deviations. Since we operate with a ($\log_2$)
149 transformed measure of fitness, the deviation caused by an i-th gene deletion is equal to
150 $d_i = rDR_i - 1$. The expected effect of multiple loci is the sum of all deviations involved,
151 $rDR_E = 1 + \sum d_i$. To predict how each of the 16 monosomic strains should perform, we summed
152 deviations caused by the individual deletions present on each chromosome (acquiring 16 values
153 of rDR_E). We summed both negative and positive values of d to account for the mentioned above
154 non-genetic variation of estimates. We then compared the predicted values of rDR_E with the
155 respective values of rDR_M, that is, estimates obtained experimentally for the actual monosomic
156 strains (**Datasheet 1**). **Fig. 2b** shows the expected and obtained values of *rDR*, epistasis is equal

157 to a difference between them. Epistasis between multiple deleterious gene deletions turned out to
158 be not only positive but also large, much larger than that observed for just pairs of deletions
159 (Jasnos and Korona, 2007). Most strikingly, some monosomic strains were expected to have a
160 negative doubling rate, i.e. were predicted to be effectively lethal, but turned out to be able to
161 proliferate. For several monosomics, and especially M4, most of the predicted mutational load
162 was canceled by epistasis. The contribution of epistasis to fitness appeared so high that it might
163 be difficult to accept without functional rationalization.
164
165 Shifts in transcriptome profiles
166 Although epistasis can be viewed in a purely abstract way, a deviation from
167 additivity/multiplicity, it must always have its biological explanation. Our attempt to find it
168 started with the isolation and quantitative examination of mRNA from the ancestral diploid strain
169 and eight randomly chosen monosomic strains. The first question was obvious: was the
170 deficiency in dose compensated by elevated expression? **Fig. 3a** shows that there was no
171 detectable increase in the intensity of transcription on the monosomic chromosomes. The linear
172 relation between the number of copies of a chromosome and the number of produced transcripts
173 has been reported for yeast, though most of the available data pertain to aneuploids with
174 excessive rather than lacking chromosomes (Larrimore et al., 2020; Torres et al., 2007). Hence,
175 neither our study nor earlier ones revealed compensation at the level of chromosome-scale
176 averages. Those averages are dependent on hundreds of genes, mostly dose-insensitive, and
177 therefore they would be insensitive to an increased expression of the genes which were important
178 but relatively few. In this experiment, we knew for which genes upregulation would be most
179 rewarding and could focus our attention on them. **Fig. 3b** shows that they were not transcribed at
180 elevated rates. Thus, neither physical underrepresentation (single copy) nor functional
181 importance (impact on growth) triggered transcriptomic compensation.
182 The availability of entire transcriptomes enables examination of the cell functioning far
183 beyond testing for compensatory expression at the affected loci. We aimed at finding any distinct
184 and functionally interpretable patterns of adjustments that could explain why the monosomics
185 performed better than expected. We found multiple statistically significant up- and
186 downregulations in transcriptomes of every analyzed monosomic strain (**Datasheet 2**). Both
187 parallelisms and incongruencies between them were visible. **Fig. 4a** shows the similarities.
188 The translational apparatus of the cytosol was on average considerably and universally
189 upregulated, as evidenced by transcripts coding for proteins building both large (e.g. *RPL28*) and
190 small (*RPS29B*) ribosomal subunits. Cytosolic proteolysis was downregulated (core proteasome
191 constituent *PRE6*). In a remarkable accord, chaperones needed to fold newly synthesized
192 peptides were upregulated (*SSB1/2*) while those required to direct destabilized chains to
193 degradation were downregulated (*SSA1, HSP82, HSP104*). Transcripts coding for mitochondrial
194 proteins were generally less abundant, with a marked decline in the expression of several genes
195 coding for the electron transport chain (**Datasheet 2**). At the same time, the expression of
196 antioxidative machinery was dampened, especially that of a chief ROS scavenger (*SOD2*).

To find transcriptomic differences, we examined groups of genes each reacting to a known signal. This raised chances for detecting statistical significance and functional divergence. In our experiment, all strains received identical outer signals. Therefore, different expression patterns would indicate different internal distortions. Indeed, as **Fig. 4b** demonstrates, substantial variation was detected within several regulons: cAMP-PKA (glucose-activated signaling), NCR (nitrogen catabolism repression), GAAC (general amino acids control), and Msn2up (activation upon a broad array of stress factors).

Discussion

The successful derivation of monosomic strains demonstrated that it is possible to obtain an a priori designed set of strains with hundreds of partially inactive genes with tens of them exerting deleterious fitness effects. It implies that the ability to remain viable despite carrying extensive mutational burdens was not restricted to assorted combinations of affected genes but would likely hold for a broad variety of them. The viability was supported by the epistatic effect which was of positive value and remarkable strength. The contribution of epistasis was probably still underestimated. It has been recently exposed that many of the single deletions with negative fitness effects had undergone compensatory evolution under recurrent propagation of the strains carrying them (Puddu et al., 2019). Therefore, some of those deletions were likely missing among our strains or were partially compensated which made their joint predicted harm lower than it would be in an unaffected collection. All those potentially missing heterozygous effects were present in the freshly derived monosomic strains biasing downward the difference between obtained and expected fitness, that is, the estimated contribution of epistasis. This caveat actually strengthens our claim of detecting the positive epistatic component that is sizable and can even offset most of the total harm associated with single negative effects.

The ascent of systems biology has raised hopes that the “statistical” and “biological” sides of epistasis can be merged coherently (Moore and Williams, 2005; Phillips, 2008). Indeed, a truly functional explanation of the measured growth effects would require understanding how the material and energetic expenditures were altered by the same mutations when they were separate or combined. Such an ultimately metabolomic interpretation could be attempted only semi-quantitatively and for much simpler systems (Molenaar et al., 2009). Regarding proteome and transcriptome, the latter has the advantage of higher accuracy and repeatability, as well as sensitivity to products of weakly expressed genes. The relation between transcriptome and proteome is generally rigid in yeast. In yeast aneuploids, the bulk of changes observed in mRNA are generally reflected as proportional shifts in both the profile of translation and mature protein composition (Larrimore et al., 2020; Pavelka et al., 2010). The relation is not perfect as, for example, disomics do have a somewhat attenuated average expression of proteins coded at the doubled chromosome, but the outcome is still much closer to doubling than parity (Dephoure et al., 2014). The post-transcriptional attenuation can be more frequent and pronounced when single genes are doubled but this is a case much different from ours (Ascencio et al., 2021). Most importantly, the yeast transcriptome is currently unparalleled in providing broad and

comprehensible insights into cell signaling and functioning under major transitions such as fast-slow growth, anabolism-catabolism, presence-absence of stress. In sum, although the analysis of mRNA obviously does not provide a full description of the cell's state, it is a sensible introduction to it.

The simultaneous upregulation of genes coding for ribosomal proteins (RP) and downregulation of those coding for subunits of the proteasome was observed in all monosomic strains and is likely providing crucial insight into the functional reaction of the cell to monosomy. An absence of a single chromosome meant halving the dose of several genes coding for the translational apparatus that resided on it while tens of others remained unaffected. The cell could not restore the required stoichiometry by targeted overexpression of the affected genes. The favorable environmental conditions signaled that translation had to be intensified but the functioning ribosomes were scarce resulting in apparently indiscriminate overproduction and withholding of degradation of all needed proteins. The reaction was inadequate and costly, but it should be seen as an attempt at *ad hoc* rebalancing, not a prepared (evolved) response. This interpretation, strongly suggested by the transcriptomic data, appears still more plausible after considering the functional diversity of the 468 genes selected as haploinsufficient. **Table 1** shows that the diversity was ample: of the one hundred Slim GO Biological Process categories, dozens could be linked to every chromosome-associated subset of deletions. The number of affected processes was higher than the number of deletions because a single deletion often belonged to several categories (Saccharomyces Genome Database). However, there was a telling common motif. The processes involved in the "protein synthesis apparatus" (our designation) were most often represented. Their predicted harm was also especially high, typically sufficient or exceeding that required to reduce the growth rate to the levels actually observed in monosomics. The distortion of biosynthesis was thus real and its relation to the observed transcriptomic reaction was probably causal, not merely coincidental.

Some of the other adjustments seen in the monosomic transcriptomes could be also linked to the dominant effect of translational inefficiency. A signal to increase biosynthesis would mobilize fermentation and curb oxidation which downregulated genes coding for the ROS-scavenging proteins. The Mns2-mediated and other stress responses were seemingly absent, contrary to previous reports (Sheltzer et al., 2012). But, among the hallmarks of stress reactions are decreased RP production and increased proteolysis (to remove destabilized proteins). These two processes were here pushed in opposite directions by the loss of RPs stoichiometry blurring the expected patterns. The non-homogeneity of reaction in other analyzed regulons—cAMP-PKA, NCR, GAAC—means that functions other than ribosome assemblage were affected seriously but differently, depending on the composition of genes made insufficient by the loss of a chromosome. The environment was the same and rich, with nothing in short supply, therefore perceived deficiency of metabolites resulted from internal distortions. **Datasheet 2** shows a very large number of differences between monosomics in the expression of single genes, the variation that would be difficult to summarize or, still more, to fully understand

in functional terms. If only some of the challenges met by individual monosomics were similar, while so many others disparate, then why was the uniformly positive epistasis observed?

A possible answer starts with the realization that the cell is an aggregate of multiple functional modules (Hartwell et al., 1999). Our monosomic strains had many different modules (recall the Slim GO categories) that were negatively affected by partially inactivating mutations. These mutations did not interact with each other directly but rather through the modules they belonged to. Mutations that affected the most critical module(s) suppressed the negative effect of those mutations that impaired other, non-limiting, modules. The latter were either less damaged or less needed under current conditions. The epiphenomenon of positive epistasis for fitness reflected the fact that not all mutations exerted their negative effects, at least not at a full scale. In our case, it is not just speculation but rather the simplest and most prudent explanation linking the growth rate and transcriptomic data. Our experimental system is in a way special: a microbial cell with multiple modules compromised but exposed to favorable conditions and thus tested for the single capacity of growing fast. However, it is also illuminating. A unicellular organism is typically tested for only a few fitness-defining functions, they would be much different under prolonged starvation. The specialized cells of a complex organism are required to uphold only some, and different, elements of life. The modularity of the cell helps to understand how so many partial genetic insufficiencies can be carried by so many different organisms without causing a drastic decline in their fitness.

Interactions within pairs of gene knock-outs have attracted much attention and some attempts to understand the uncovered variety of fitness effects have relied on the concept of cellular modularity (Costanzo et al., 2020; Segrè et al., 2005; Szappanos et al., 2011). High-order epistasis for fitness, arising from interactions between at least several mutations, has been often mentioned in the context of "diminished returns" of consecutive beneficial variants (Barrick et al., 2009; Chou et al., 2011; Khan et al., 2011; Kryazhimskiy et al., 2014). It has been proposed that the pattern emerges from interactions of mutations through some 'global' phenotypic interface, e.g., fitness (MacLean et al., 2010; Perfeito et al., 2014; Schoustra et al., 2016). However, a similar overall effect could be theoretically generated by the entirety of 'idiosyncratic' interactions, without any intermediating factors (Lyons et al., 2020; Reddy and Desai, 2021). Indeed, this has been demonstrated experimentally, at least for a selected and moderately large set of mutations (Bakerlee et al., 2022). Finally, the diminishing returns epistasis of beneficial mutations has been attributed to cellular modularity by postulating that the contribution of each functional module to fitness must have its upper limit (Wei and Zhang, 2019). Considering that the negative epistasis between multiple positive effects can result from different mechanisms, we do not insist that the proposed by us explanation of positive epistasis between multiple negative effects is the only one possible. However, it can be especially applicable when the deleterious mutations are really numerous and distributed widely, though not necessarily evenly, across many cellular subsystems.

Materials and Methods

Single gene deletion strains

1.1. Selection of single gene deletions with a possible effect of haploinsufficiency

Deutschbauer *et al.* have assayed a complete collection of heterozygous single gene deletion strains and identified a total of 184 genes, 98 essential and 86 non-essential, as haploinsufficient for growth in rich medium, YPD (Deutschbauer et al., 2005). We included this set of genes in the present study. Using a different technique, Marek *et al*. have tested al1 142 essential heterozygous single-gene deletions and 946 non-essential ones selected as likely non-neutral for growth (Marek and Korona, 2016). We reviewed the latter study and, setting a level of false discovery rate at 0.15, accepted as many as 404 genes, 256 essential and 148 non-essential, as potentially haploinsufficient. The two sets obtained in two different studies, 184 and 404, overlapped in 112 cases. The overlap was clearly higher than expected, 14.3, if the two sets were just random samples from among 5,200 yeast genes. On the other hand, it was limited and suggested new growth assays were desirable. The new assays are described below, they involved all unique strains identified in the two studies minus 5 which were not present in our present strain collections and another 3 which were dropped as superfluous for the described below orthogonal design of experimental blocks. (They were also the 3 least promising based on the former assays.) **Datasheet 1** lists the strains.

1.2. Control for single deletion strains

To correctly quantify the predictably small negative growth effects introduced by heterozygous single-deletion strains, an unbiased and precise estimate of a wild-type phenotype is needed. In the present study, we sought to accomplish this by setting not a single but multiple strains as a control. The reason was that the used here gene deletions were constructed over several years by multiple laboratories and were then handled with repeated rounds of propagation that could result in genetic divergence. We therefore considered it risky to choose a single strain as a control for all others. We looked for a group of strains that would be indistinguishable in terms of growth rate suggesting that they have acquired genetic alterations affecting this trait. In the case of non-essential genes, we reviewed the Saccharomyces Genome Database and found 25 ORFs termed “dubious”, at present nearly sure to be false ORFs, which were located between other ORFs and no closer to their START or STOP codons than 100 bp. Heterozygous strains carrying deletions of these genes were assayed for doubling rate in a way specific to this study (described below). After replicated assays, 16 deletion strains closest to the medium growth performance, and statistically not different from each other, were selected as the control ones. Knowing that the non-essential and essential strains differed somewhat in their origin and subsequent handling (Brachmann et al., 1998), we decided to derive a separate set of control strains for the latter. We selected 32 essential genes which were in the very center of a single, strong and narrow modal peak of the frequency distribution of estimates collected for the whole

collection of heterozygous essentials (Marek and Korona, 2016). Again, after replicated tests of growth rate, 16 strains closest to the median value and not different from each other were selected to constitute the final control for essential gene deletions. Control strains of both groups are listed in **Datasheet 1**.

Monosomic strains

2.1. Parents of monosomic strains

In a former study, we used 32 strains that had one counter-selectable marker (*URA3*) close to the center of each of the 32 chromosomal arms and a drug resistance marker (*kan*) close to a centromere (Tutaj et al., 2022). Pairs of strains with the same centromere marker and the counter-selectable markers residing on either the left or right arm of the same chromosome were mated with each other. The resulting diploids were sporulated and tetrads dissected to get triple-marked haploid genotypes, *URA3-kan-URA3*. The latter were mated with a standard BY haploid strain of the opposite mating type. In the final set of 16 diploid strains, each strain had one chromosome triple-marked while its homolog and the rest of the 15 chromosome pairs were isogenic with the diploid strain BY4743.

2.2. Derivation and verification of monosomic strains

The diploid strains with triple-marked chromosomes were grown overnight in synthetic complete medium (SC) and then 50 to 500 µl samples of the resulting cultures were overlaid on standard 5-FOA (5-fluoroorotic acid) plates. Emerging colonies were transferred onto new 5-FOA plates and YPD plates with 200 mg/ml of geneticin. The goal was to identify variants that were able to grow on the 5-FOA but not geneticin plates as this indicated that all three marker genes were possibly lost together with an entire chromosome. Colonies identified in this way were often of different sizes suggesting that they were genetically heterogeneous. The next criterion was to find variants that would form visibly smaller colonies than those of the parental strain but rarely, though regularly, produce colonies similar to the latter. Such strains were grown as replicate small cultures (5 to 100 µl dependent on particular monosomic strain), tested for negligible frequency of cells forming large colonies, and collected into larger samples enabling isolation of DNA at amounts sufficient for the next generation sequencing. Monosomy was considered confirmed when the number of reads was halved for the whole stretch of a single, and the expected one, chromosome. Although simple, this protocol required multiple attempts to be completed for some chromosomes as few colonies tended to appear on the 5-FOA plates, most of them remained resistant to geneticin and those which passed these two criteria did not show the required reversibility, that is, the tendency to return occasionally to normal growth in apparently one step. Even if all these phenotypic criteria were met, the sequencing occasionally uncovered genomes other than those of pure monosomics, that is, with the whole and only single-chromosome removed. Nevertheless, once confirmed, the monosomic strains could have been propagated reliably on rich and synthetic media, including that with 5-FOA, as long as the recurrent emergence of fast-growing colonies was monitored and countered.

396
397 *2.3. Control for monosomic strains*
398 The monosomic strains were all derived by us and the derivation involved our stock of haploid
399 BY4741 and BY4742 strains. These two were then crossed to obtain a diploid BY4743, devoid
400 of the *URA3*MX4 and *kan*MX4 cassettes, and then used as a control in growth assays of the
401 monosomic strains.
402
403 Estimation of *DR* and *rDR*
404 The collection of single gene deletion strains was arrayed on 6 flat-bottom 8×12 well titration
405 plates with 150 µl aliquots per well. Within each plate, the first and last well contained clean
406 YPD medium, rows 3 and 10 hosted control strains, and deletion strains occupied the rest of the
407 plate. Plates were filled with either essential or non-essential deletions accompanied by the
408 respective 16 control strains mentioned above. One plate contained both essential and non-
409 essential deletions together with 8 essential and 8 non-essential control strains. Plates were
410 inoculated from thawed samples at 1-5% and kept non-agitated for 48 hours at 30 °C when they
411 reached approximately similar densities of stationary phase cells. Such conditioned micro-
412 cultures were used to inoculate plates with fresh YPD at 0.5% and kept at 30 °C with 1,000 rpm
413 agitation. The cultures were tested for OD (600 nm) every 0.5 h with a TECAN Infinity reader.
414 Four independent replicates of the measurements, starting with independent conditionings, were
415 carried out. OD reads were used to calculate *DR* (doubling rate). To get *rDR* (relative doubling
416 rate), every *DR* estimate of an experimental strain was divided by an average *DR* of control
417 strains residing on the same plate. In the case of the monosomic strains, the whole protocol was
418 analogous except that all experimental and control strains were held within one plate. The
419 cultures of monosomic strains used in this assay were tested to contain less than 1% of fast-
420 growing cells at the time of OD measurements.
421
422 Analysis of DNA and RNA
423 An initial step in preparing for both the DNA and RNA analysis was to collect samples of
424 monosomic cells that would be nearly free of the fast-growing revertant cells. Individual
425 monosomic strains were grown in YPD at 30 °C up to stationary phase as replicate micro-
426 cultures (5 to 100 µl). The latter were serially diluted and plated to test for the appearance of
427 large colonies suggesting the rise of compensatory mutations. The micro-cultures in which
428 colonies typical for a particular monosomic strain constituted more than 99% were pooled
429 together. Such tested stationary cultures of monosomic cells were directly used to extract DNA
430 as a template for high-coverage sequencing (PE 150, expected read depth ~80). The resulting
431 reads were mapped, using bowtie2 (Langmead and Salzberg, 2012), along standard sequences of
432 yeast chromosomes: Ensembl release 100, *S. cerevisiae* genome R64-1-1. Duplicated reads were
433 marked with MarkDuplicates (Picard Toolkit 2019. Broad Institute, GitHub). Samtools (1.15.1)
434 were used for BAM files sorting, indexing and coverage analysis (Danecek et al., 2021).

In the case of RNA, the tested for purity cultures of monosomic cells were transferred to fresh YPD and incubated with agitation at 30 °C for 4 hours. Total RNA was then extracted with the RiboPure™ RNA Purification Kit. Three replicas of the monosomic and the control BY4743 strain were prepared in this way. Libraries preparation and PE 150 sequencing was carried out by Novagene. About 20 mln read pairs were obtained per sample. Quality control of the reads was performed with fastQC v0.11.9 (Andrew, 2010). The RNA reads were mapped to the above-specified standard sequence with Hisat2 v2.1.0 (Kim et al., 2015). The resulting alignment files were sorted and indexed with samtools (1.9). Transcript quantification was performed with cuffquant/cuffnorm v2.2.1 (Trapnell et al., 2012). Gene count data normalization ("TMM" method) and differential expression analysis (exact test) were performed in the EdgeR test(Robinson et al., 2010).

Acknowledgments

We thank J. Bobula and A. Pirog for their experimental assistance.

References

Andrew S. 2010. A quality control tool for high throughput sequence data. *Fast QC* **390**:391.

Ascencio D, Diss G, Gagnon-Arsenault I, Dubé AK, DeLuna A, Landry CR. 2021. Expression attenuation as a mechanism of robustness against gene duplication. *Proc Natl Acad Sci U S A* **118**:1–10. doi:10.1073/pnas.2014345118

Bakerlee CW, Nguyen Ba AN, Shulgina Y, Rojas Echenique JI, Desai MM. 2022. Idiosyncratic epistasis leads to global fitness–correlated trends. *Science (1979)* **376**:630–635. doi:10.1126/science.abm4774

Barrick JE, Yu DS, Yoon SH, Jeong H, Oh TK, Schneider D, Lenski RE, Kim JF. 2009. Genome evolution and adaptation in a long-term experiment with Escherichia coli. *Nature* **461**:1243–1247. doi:10.1038/nature08480

Beach RR, Ricci-Tam C, Brennan CM, Moomau CA, Hsu P hsin, Hua B, Silberman RE, Springer M, Amon A. 2017. Aneuploidy Causes Non-genetic Individuality. *Cell* **169**:229-242.e21. doi:10.1016/j.cell.2017.03.021

Brachmann CB, Davies A, Cost GJ, Caputo E, Li J, Hieter P, Boeke JD. 1998. Designer deletion strains derived from Saccharomyces cerevisiae S288C: A useful set of strains and plasmids for PCR-mediated gene disruption and other applications. *Yeast* **14**:115–132. doi:10.1002/(SICI)1097-0061(19980130)14:2<115::AID-YEA204>3.0.CO;2-2

Chou HH, Chiu HC, Delaney NF, Segrè D, Marx CJ. 2011. Diminishing returns epistasis among beneficial mutations decelerates adaptation. *Science (1979)* **332**:1190–1192. doi:10.1126/science.1203799

Costanzo M, Baryshnikova A, Bellay J, Kim Y, Spear ED, Sevier CS, Ding H, Koh JL, Toufighi K, Mostafavi S, Prinz J, St Onge RP, VanderSluis B, Makhnevych T, Vizeacoumar FJ, Alizadeh S, Bahr S, Brost RL, Chen Y, Cokol M, Deshpande R, Li Z, Lin Z-Y, Liang W, Marback M, Paw J, San Luis B-J, Shuteriqi E, Hin Yan Tong A, van Dyk N, Wallace IM, Whitney JA, Weirauch MT, Zhong G, Zhu H, Houry WA, Brudno M, Ragibizadeh S, Papp B, Pál C, Roth FP, Giaever G, Nislow C, Troyanskaya OG, Bussey H, Bader GD, Gingras

479 A-C, Morris QD, Kim PM, Kaiser CA, Myers CL, Andrews BJ, Boone C. n.d. The Genetic
480 Landscape of a Cell. Science (*2010)* **327**:425-432. Doi: 10.1126/science.1180823
481 Danecek P, Bonfield JK, Liddle J, Marshall J, Ohan V, Pollard MO, Whitwham A, Keane T,
482 McCarthy SA, Davies RM, Li H. 2021. Twelve years of SAMtools and BCFtools.
483 *Gigascience* **10**:1–4. doi:10.1093/gigascience/giab008
484 Dephoure N, Hwang S, O'Sullivan C, Dodgson SE, Gygi SP, Amon A, Torres EM. 2014.
485 Quantitative proteomic analysis reveals posttranslational responses to aneuploidy in yeast.
486 *Elife* **3**:1–27. doi:10.7554/eLife.03023
487 Deutschbauer Adam M, Jaramillo DF, Proctor M, Kumm J, Hillenmeyer ME, Davis RW, Nislow
488 C, Giaever G. 2005. Mechanisms of haploinsufficiency revealed by genome-wide profiling
489 in yeast. *Genetics* **169**:1915–1925.
490 Deutschbauer Adam M., Jaramillo DF, Proctor M, Kumm J, Hillenmeyer ME, Davis RW,
491 Nislow C, Giaever G. 2005. Mechanisms of haploinsufficiency revealed by genome-wide
492 profiling in yeast. *Genetics* **169**:1915–1925. doi:10.1534/genetics.104.036871
493 Giaever G, Chu AM, Ni L, Connelly C, Riles L, Vé ronneau S, Dow S, Lucau-Danila A,
494 Anderson K, André B, Arkin AP, Astromoff A, el Bakkoury M, Bangham R, Benito R,
495 Brachat S, Campanaro S, Curtiss M, Davis K, Deutschbauer A, Entian K-D, Flaherty P,
496 Foury F, Garfinkel DJ, Gerstein M, Gotte D, Gü ldener U, Hegemann JH, Hempel S,
497 Herman Z, Jaramillo DF, Kelly DE, Kelly SL, Kö tter P, LaBonte D, Lamb DC, Lan N,
498 Liang H, Liao H, Liu L, Luo C, Lussier M, Mao R, Menard P, Loon Ooi S, Revuelta JL,
499 Roberts CJ, Rose M, Ross-Macdonald P, Scherens B, Schimmack G, Shafer B, Shoemaker
500 DD, Sookhai-Mahadeo S, Storms RK, Strathern JN, Valle G, Voet M, Volckaert G, Wang
501 C, Ward TR, Wilhelmy J, Winzeler EA, Yang Y, Yen G, Youngman E, Yu K, Bussey H,
502 Boeke JD, Snyder M, Philippsen P, Davis RW, Johnston M. 2002. Functional profiling of
503 the Saccharomyces cerevisiae genome. *Nature* **418**:387-391.
504 Hartwell LH, Hopfield JJ, Leibler S, Murray AW. 1999. From molecular to modular cell biology
505 **402**:47–52. *Nature* **402**:C47–C5
506 Henn BM, Botigué LR, Bustamante CD, Clark AG, Gravel S. 2015. Estimating the mutation
507 load in human genomes. *Nat Rev Genet* **16**:333–43. doi:10.1038/nrg3931
508 J. A, Crow JF, Kimura M. 1971. An Introduction to Population Genetics Theory. *Population*
509 *(French Edition)* **26**:977. doi:10.2307/1529706
510 Jasnos L, Korona R. 2007. Epistatic buffering of fitness loss in yeast double deletion strains. *Nat*
511 *Genet* **39**:550–554. doi:10.1038/ng1986
512 Khan AI, Dinh DM, Schneider D, Lenski RE, Cooper TF. 2011. Negative epistasis between
513 beneficial mutations in an evolving bacterial population. *Science (1979)* **332**:1193–1196.
514 doi:10.1126/science.1203801
515 Kim D, Langmead B, Salzberg SL. 2015. HISAT: a fast spliced aligner with low memory
516 requirements. *Nat Methods* **12**:357–360.
517 Kryazhimskiy S, Rice DP, Jerison ER, Desai MM. 2014. Global epistasis makes adaptation
518 predictable despite sequence-level stochasticity. *Science (1979)* **344**:1519–1522.
519 doi:10.1126/science.1250939
520 Langmead B, Salzberg SL. 2012. Fast gapped-read alignment with Bowtie 2. *Nat Methods* **9**:357.
521 Larrimore KE, Barattin-Voynova NS, Reid DW, Ng DTW. 2020. Aneuploidy-induced
522 proteotoxic stress can be effectively tolerated without dosage compensation, genetic
523 mutations, or stress responses. *BMC Biol* **18**:117. doi:10.1186/s12915-020-00852-x

Lyons DM, Zou Z, Xu H, Zhang J. 2020. Idiosyncratic epistasis creates universals in mutational effects and evolutionary trajectories. *Nat Ecol Evol* **4**:1685–1693. doi:10.1038/s41559-020-01286-y

MacArthur DG, Balasubramanian S, Frankish A, Huang N, Morris J, Walter K, Jostins L, Habegger L, Pickrell JK, Montgomery SB, Albers CA, Zhang ZD, Conrad DF, Lunter G, Zheng H, Ayub Q, DePristo MA, Banks E, Hu M, Handsaker RE, Rosenfeld JA, Fromer M, Jin M, Mu XJ, Khurana E, Ye K, Kay M, Saunders GI, Suner M-M, Hunt T, Barnes IHA, Amid C, Carvalho-Silva DR, Bignell AH, Snow C, Yngvadottir B, Bumpstead S, Cooper DN, Xue Y, Romero IG, Wang J, Li Y, Gibbs RA, McCarroll SA, Dermitzakis ET, Pritchard JK, Barrett JC, Harrow J, Hurles ME, Gerstein MB, Tyler-Smith C. 2012. A Systematic Survey of Loss-of-Function Variants in Human Protein-Coding Genes. *Science (1979)* **335**:823–828. doi:10.1126/science.1215040

MacLean RC, Perron GG, Gardner A. 2010. Diminishing returns from beneficial mutations and pervasive epistasis shape the fitness landscape for rifampicin resistance in Pseudomonas aeruginosa. *Genetics* **186**:1345–1354. doi:10.1534/genetics.110.123083

Marek A, Korona R. 2016. Strong dominance of functional alleles over gene deletions in both intensely growing and deeply starved yeast cells. *J Evol Biol* **29**:1836–1845. doi:10.1111/jeb.12917

Molenaar D, van Berlo R, de Ridder D, Teusink B. 2009. Shifts in growth strategies reflect tradeoffs in cellular economics. *Mol Syst Biol*. doi:10.1038/msb.2009.82

Moore JH, Williams SM. 2005. Traversing the conceptual divide between biological and statistical epistasis: Systems biology and a more modern synthesis. *BioEssays*. doi:10.1002/bies.20236

Moore L, Cagan A, Coorens THH, Neville MDC, Sanghvi R, Sanders MA, Oliver TRW, Leongamornlert D, Ellis P, Noorani A, Mitchell TJ, Butler TM, Hooks Y, Warren AY, Jorgensen M, Dawson KJ, Menzies A, O'Neill L, Latimer C, Teng M, van Boxtel R, Iacobuzio-Donahue CA, Martincorena I, Heer R, Campbell PJ, Fitzgerald RC, Stratton MR, Rahbari R. 2021. The mutational landscape of human somatic and germline cells. *Nature* **597**:381–386. doi:10.1038/s41586-021-03822-7

Ohnuki S, Ohya Y. 2018. High-dimensional single-cell phenotyping reveals extensive haploinsufficiency. *PLoS Biol* **16**:e2005130. doi:10.1371/journal.pbio.2005130

Pavelka N, Rancati G, Zhu J, Bradford WD, Saraf A, Florens L, Sanderson BW, Hattem GL, Li R. 2010. Aneuploidy confers quantitative proteome changes and phenotypic variation in budding yeast. *Nature* **468**:321–325. doi:10.1038/nature09529

Perfeito L, Sousa A, Bataillon T, Gordo I. 2014. Rates of fitness decline and rebound suggest pervasive epistasis. *Evolution (N Y)* **68**:150–162. doi:10.1111/evo.12234

Peter J, de Chiara M, Friedrich A, Yue JX, Pflieger D, Bergström A, Sigwalt A, Barre B, Freel K, Llored A, Cruaud C, Labadie K, Aury JM, Istace B, Lebrigand K, Barbry P, Engelen S, Lemainque A, Wincker P, Liti G, Schacherer J. 2018. Genome evolution across 1,011 Saccharomyces cerevisiae isolates. *Nature* **556**:339–344. doi:10.1038/s41586-018-0030-5

Phillips PC. 2008. Epistasis - The essential role of gene interactions in the structure and evolution of genetic systems. *Nat Rev Genet*. doi:10.1038/nrg2452

Puddu F, Herzog M, Selivanova A, Wang S, Zhu J, Klein-Lavi S, Gordon M, Meirman R, Millan-Zambrano G, Ayestaran I, Salguero I, Sharan R, Li R, Kupiec M, Jackson SP. 2019. Genome architecture and stability in the Saccharomyces cerevisiae knockout collection. *Nature* **573**:416–420. doi:10.1038/s41586-019-1549-9

570 Reddy G, Desai MM. 2021. Global epistasis emerges from a generic model of a complex trait.
571 *Elife* **10**:1–36. doi:10.7554/eLife.64740
572 Reid RJD, Sunjevaric I, Voth WP, Ciccone S, Du W, Olsen AE, Stillman DJ, Rothstein R. 2008.
573 Chromosome-Scale Genetic Mapping Using a Set of 16 Conditionally Stable
574 *Saccharomyces cerevisiae* Chromosomes. *Genetics* **180**:1799–1808.
575 doi:10.1534/genetics.108.087999
576 Robinson MD, McCarthy DJ, Smyth GK. 2010. edgeR: a Bioconductor package for differential
577 expression analysis of digital gene expression data. *Bioinformatics* **26**:139–140.
578 Schoustra S, Hwang S, Krug J, de Visser JAGM. 2016. Diminishing-returns epistasis among
579 random beneficial mutations in a multicellular fungus. *Proceedings of the Royal Society B:*
580 *Biological Sciences* **283**. doi:10.1098/rspb.2016.1376
581 Segrè D, DeLuna A, Church GM, Kishony R. 2005. Modular epistasis in yeast metabolism. *Nat*
582 *Genet* **37**:77–83. doi:10.1038/ng1489
583 Sheltzer JM, Torres EM, Dunham MJ, Amon A. 2012. Transcriptional consequences of
584 aneuploidy. *Proc Natl Acad Sci U S A* **109**:12644–12649. doi:10.1073/pnas.1209227109
585 Sliwa P, Korona R. 2005. Loss of dispensable genes is not adaptive in yeast.
586 Steinmetz LM, Scharfe C, Deutschbauer AM, Mokranjac D, Herman ZS, Jones T, Chu AM,
587 Giaever G, Prokisch H, Oefner PJ, Davis RW. 2002. Systematic screen for human disease
588 genes in yeast. *Nat Genet* **31**:400–404. doi:10.1038/ng929
589 Sui Y, Qi L, Wu J-K, Wen X-P, Tang X-X, Ma Z-J, Wu X-C, Zhang K, Kokoska RJ, Zheng D-
590 Q. 2020. Genome-wide mapping of spontaneous genetic alterations in diploid yeast cells.
591 *Proceedings of the National Academy of Sciences* **117**:28191–28200.
592 Szamecz B, Boross G, Kalapis D, Kovács K, Fekete G, Farkas Z, Lázár V, Hrtyan M, Kemmeren
593 P, Groot Koerkamp MJA, Rutkai E, Holstege FCP, Papp B, Pál C. 2014. The genomic
594 landscape of compensatory evolution. *PLoS Biol* **12**:e1001935.
595 doi:10.1371/journal.pbio.1001935
596 Szappanos B, Kovács K, Szamecz B, Honti F, Costanzo M, Baryshnikova A, Gelius-Dietrich G,
597 Lercher MJ, Jelasity M, Myers CL, Andrews BJ, Boone C, Oliver SG, Pál C, Papp B. 2011.
598 An integrated approach to characterize genetic interaction networks in yeast
599 metabolismNature Genetics. pp. 656–662. doi:10.1038/ng.846
600 Torres EM, Sokolsky T, Tucker CM, Chan LY, Boselli M, Dunham MJ, Amon A. 2007. Effects
601 of aneuploidy on cellular physiology and cell division in haploid yeast. *Science (1979)*
602 **317**:916–924. doi:10.1126/science.1142210
603 Trapnell C, Roberts A, Goff L, Pertea G, Kim D, Kelley DR, Pimentel H, Salzberg SL, Rinn JL,
604 Pachter L. 2012. Differential gene and transcript expression analysis of RNA-seq
605 experiments with TopHat and Cufflinks. *Nat Protoc* **7**:562.
606 Tutaj H, Pirog A, Tomala K, Korona R. 2022. Genome-scale patterns in the loss of
607 heterozygosity incidence in Saccharomyces cerevisiae. *Genetics* **221**.
608 doi:10.1093/genetics/iyac032
609 Wei X, Zhang J. 2019. Patterns and Mechanisms of Diminishing Returns from Beneficial
610 Mutations. *Mol Biol Evol* **36**:1008–1021. doi:10.1093/molbev/msz035
611 Zhu YO, Siegal ML, Hall DW, Petrov DA. 2014. Precise estimates of mutation rate and
612 spectrum in yeast. *Proc Natl Acad Sci U S A* **111**. doi:10.1073/pnas.1323011111
613
614
615
616

617 Table 1. Yeast Slim GO Biological Process categories of the tested deletions and the predicted and
618 observed relative doubling rate of the monosomic strains.
619

Monosomic strain	**M1**	**M2**	**M3**	**M8**	**M10**	**M11**	**M14**	**M16**
Subsets of deletions mapping to chromosomes								
Number of GO Slim Biological Process categories	25	47	11	27	39	33	34	57
Number of unique genes	6	40	11	20	31	19	24	41
Number of genes affecting categories constituting PSA (protein synthesis apparatus):								
- rRNA processing	1	5	3	7	4	5	8	11
- ribosome large subunit biogenesis		1	1			4	6	7
- ribosome small subunit biogenesis	1	4	2	4	3	1	2	5
- ribosomal assembly	1	1	1	1		2	1	2
- ribosome subunit export from nucleus				1	2	3	2	4
- cytoplasmic translation	1	9		5	4	5	3	5
- translational initiation	1				2			
- regulation of translation		2	2					
Total number of unique PSA genes	1	13	5	8	10	7	12	14
Relative doubling rate (rDR)								
- predicted from the total load of deletions (Fig. 2b)	0.85	-0.95	0.66	0.27	-0.82	-0.33	-0.04	-1.52
- predicted from the PSA deletions	0.95	0.37	0.78	0.63	0.22	0.49	0.22	-0.07
- observed in monosomic strains	0.96	0.60	0.63	0.61	0.49	0.60	0.63	0.58

620
621
622
623
624
625

626 **Figure 1 (main text)**
627
628

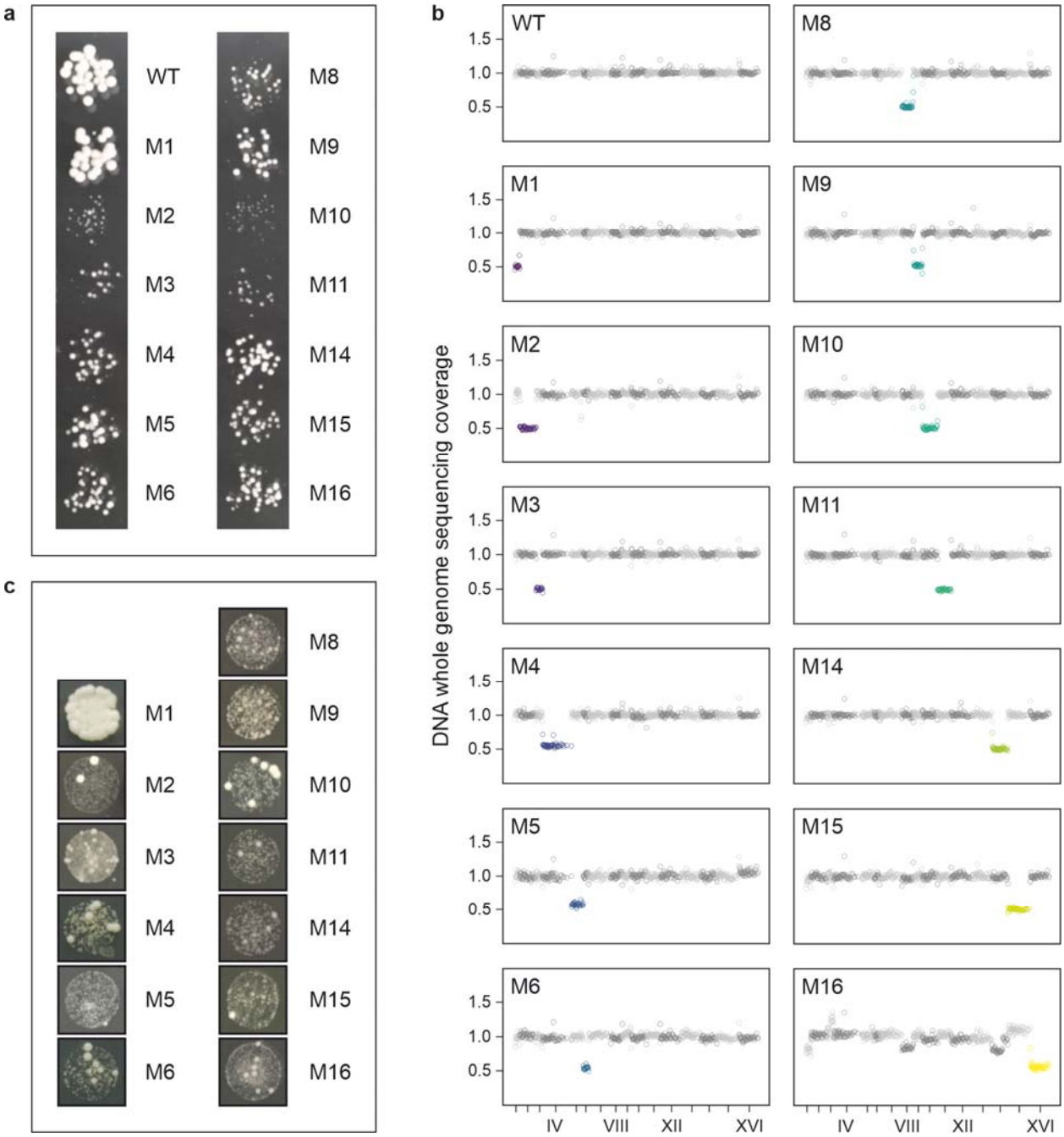

629
630
631 **Fig. 1. Diploid yeast strains lacking single chromosomes (monosomics).** (**a**) Representative
632 colonies of wild-type diploid (WT) and monosomic mutant strains (M1...M16) when grown
633 together for 24 hours at 30 °C on agar-solidified YPD medium. (**b**) DNA whole genome
634 sequencing coverage. (**c**) Examples of large colonies emerging among the small monosomic
635 ones.
636

637 **Figure 2 (main text)**
638
639

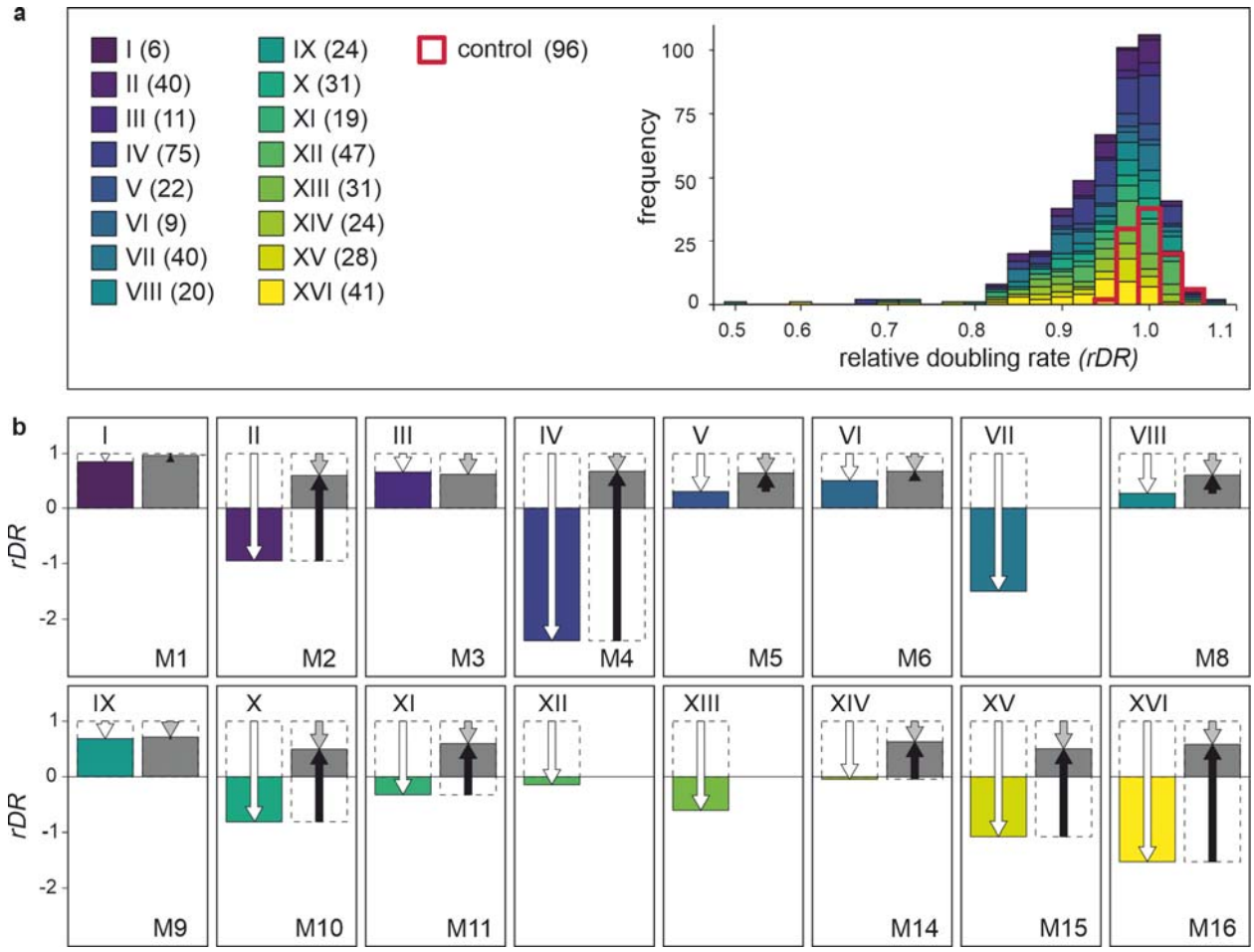

640 **Fig. 2. Contribution of positive epistasis to fitness of monosomics.** (**a**) Growth performance of
641 heterozygous single-gene deletion strains tested in this study. Left: list of chromosomes with
642 numbers of assayed deletion strains. Right: frequency distribution of *rDR* (doubling rate related
643 to that of the control). (**b**) Growth performance of monosomics. Colored bars represent expected
644 performance calculated as a sum of the single-gene effects per chromosome, $rDR_E=1+\sum d_i$, where
645 $d_i=rDR_i-1$ (deviation from the control). Gray bars show the observed performance of
646 monosomic strains, rDR_M. White arrows mark the expected departure from wild-type fitness
647 (expected genetic load), gray the observed one. Black arrows show the extent and direction of
648 epistasis. Three monosomics were not included in these assays (see the main text).

649

650

651

652 **Figure 3 (main text)**

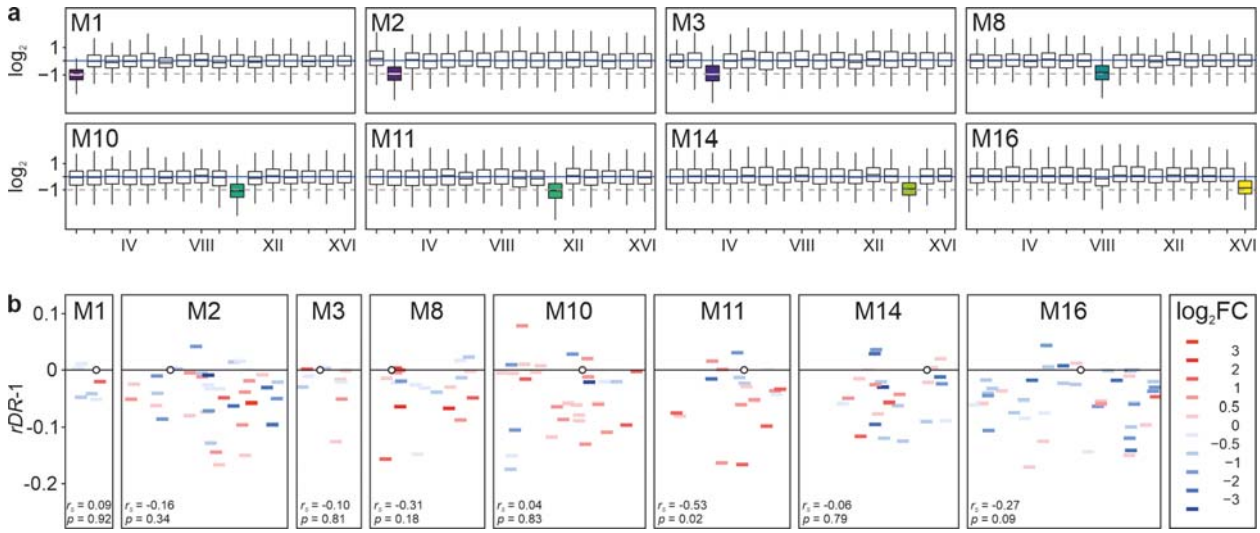

653

654

655 **Fig. 3. Absence of transcriptional compensation in monosomic strains.** (**a**) Halved RNA
656 production on monosomic chromosomes. For every ORF, the obtained number of RNA-seq
657 reads was divided by the number expected for it under expression being constant over an entire
658 genome. (**b**) Expression under monosomy vs. single-deletion fitness (*rDR*). X-axis: the effect of
659 monosomy on a particular mRNA level was calculated as $\log_2$ fold change relative to the diploid
660 control and displayed as a color-coded bar at its chromosomal position (the width of a box
661 reflects chromosome length). The shifts in expression at the monosomic chromosomes were
662 calculated after taking into account that the gene dose was halved there. Y-axis: the difference in
663 *rDR* between a single gene deletion strain and the control, *d*=*rDR*-1. Pairs of estimates were
664 tested for rank correlation; shown are Spearman's coefficients and *p*-values (not corrected for the
665 multiplicity of comparisons).

666

667

668

669

670
671
672 **Figure 4 (main text)**
673
674

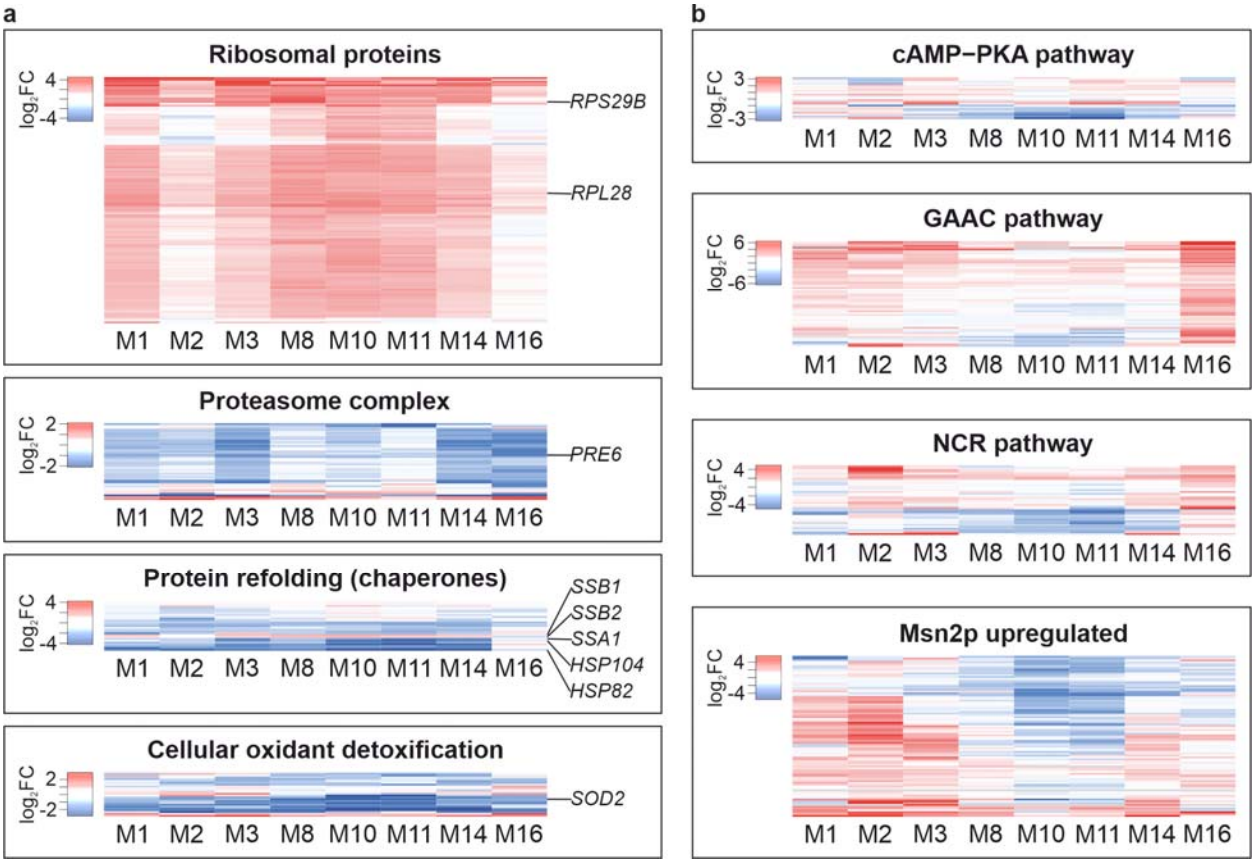

675

676 **Fig. 4. Parallel and divergent shifts in transcriptomes of monosomic strains.** Heat maps
677 show monosomic mRNA frequencies divided by respective diploid (control) ones. (**a**) Gene
678 Ontology categories selected to demonstrate similarities in transcriptional profiles of monosomic
679 strains. (**b**) Regulons demonstrating differences in gene expression between monosomic strains.
680 Expanded versions of all panels can be found in **Supplementary Figure S1**.

681
682
683
684

Additional information

Funding
National Science Centre of Poland grant NCN 2017/25/B/NZ2/01036 (RK)
National Science Centre of Poland grant NCN 2014/13/B/NZ8/04668 (KT)
Jagiellonian University grant DS/MND/WB/INoS/10/2018 (HT)

Author contributions
Conceptualization: HT, RK
Experimental design: HT, KT, RK
Experiments: HT, RK
Analysis: HT, KT, RK
Visualization: HT
Writing – original draft: RK
Writing – review & editing: HT, RK

Competing interests
The authors declare no competing interests.

Additional files

Data availability
All data generated or analyzed during this study are included in this published article (and its supplementary information files) or are deposited in the BioProject and GEO (Gene Expression Omnibus) public databases. Accession numbers can be provided upon request.

Datasheet 1 (separate Excel file)

Datasheet 2 (separate Excel file)

720 # Supplementary Materials

721

722 **Supplementary Text 21**

723 **Supplementary Figure S1 . . . . . 24**

724 **Supplementary Figure S2 . . . . . 27**

725

726

727 **Supplementary Text**

728 Transient monosomy of chromosomes VII and XIII

729 The procedure of isolating monosomics described in Material and Methods was applied in the
730 same way to all strains with marked chromosomes, including both VII and XIII. For both of
731 them, we tended to get Ura^- colonies (on 5-FOA agars) which were mostly large (wild-type size)
732 with small ones amounting to a few percent of all isolates. Looking for prospective monosomics,
733 we initially concentrated on the small colonies. Of no less than 100 isolates for each parent
734 strain, not a single one met our criteria. Most were kan^R and none of the remaining produced
735 small and largely uniform colonies which would tend to revert to wild-type growth. Despite
736 these non-encouraging signs, two of the most promising candidates for each chromosome were
737 sequenced. Complex polyploidies instead of regular monosomy were detected in these trials.

738 We then examined the dominating large Ura^- colonies. They were emerging at median
739 frequencies of 3.1E−06 and 6.3E−06 for chromosomes VII and XIII, respectively. (Number of
740 colonies divided by the number of cells plated on 5-FOA.) For each parental strain, 108 colonies,
741 collected from several separately inoculated selective agars, were taken at random for further
742 assays. All these isolates grew fast when re-streaked. Only 2 of those derived from the strain
743 hosting marked chromosome VII turned out to be kan^R, none in the case of chromosome XIII. To
744 interpret these results, it could be useful to recall that the *URA3* marker was placed in the middle
745 of both the left and right chromosomal arms while *kan* occupied one of ORFs closest to a
746 centromere:

747 telomere—*URA3*—*kan*—*URA3*—telomere.

748 Its homolog was free of all three markers. In principle, two mitotic cross-overs, between
749 telomere and *URA3*, on every arm, could produce one progeny cell with two marker-free

750 chromosomes. It would be a regular diploid and thus of the wild-type growth rate. There are two
751 arguments against this suggestion. First, double cross-over between *URA3* and *kan* would be
752 similarly frequent and therefore cells lacking *URA3* but retaining *kan* would not be as rare as it
753 was observed here. Second, we measured the frequency of crossing-over on the two
754 chromosomes in our earlier study (Tutaj et al., 2022). Based on our estimates, two simultaneous
755 cross-overs located within the distal halves of the arms of chromosomes VII and XIII would
756 happen at a rate of 1.1E−08 and 7.9E−09, respectively, which is about two orders of magnitude
757 lower than observed.

758 The fast-growing and marker-free isolates were then subjected to sporulation and tetrad
759 dissection. For every chromosome, 8 isolates were selected at random and at least 10 tetrads
760 were dissected. In each of the16 assayed strains, tetrads with four viable haploids constituted a
761 clear majority as expected for the products of meiosis with a regular diploid cell. Two of each 8
762 so analyzed strains were further tested in high-coverage DNA sequencing. No sequences of the
763 two markers or the MX4 cassette that hosted them were found. The three loci in question
764 contained only the expected wild-type sequences with a coverage typical for the rest of a
765 genome, that is diploid (**Supplementary Figure S2**).

766 To summarize, we did not find a single slow-growing monosomic strain for
767 chromosomes VII and XIII even though we were looking for them especially intensely. The
768 regularly arising fast-growing isolates with the searched phenotype were highly unlikely to result
769 from recombinational events, such as a double cross-over. They were normal diploids with the
770 chromosomes in question having the phenotypic alleles and DNA sequences characteristic of the
771 non-marked homologs. These findings imply that marked chromosomes were lost and their non-
772 marked homologs underwent endoreduplication.

773 <u>The unsuitability of chromosome XII for monosomy research</u>

774 The parent strain with triple-marked chromosome XII tended to produce unusually numerous
775 colonies on the selective 5-FOA agars, mostly as large as those of regular diploid strains. We did
776 not analyze those large colonies because we considered them to be likely produced by
777 recombination and thus unrelated to monosomy. This chromosome contains the only yeast rDNA
778 region which is long for about 1 Mb and is known to be a strong recombination hotspot.
779 Therefore, the quantitative arguments excluding double cross-overs, developed for chromosomes
780 VII and XIII, were inapplicable here. Small colonies were also more numerous than in the case

781 of other strains. The tests of markers and growth rate reversibility were applied to several
782 hundred of them but failed in nearly all trials. A few most promising isolates were sequenced and
783 none of them revealed the searched regular monosomy. We decided to stop our search of M12 at
784 this point because the presence of rDNA made it impracticable.

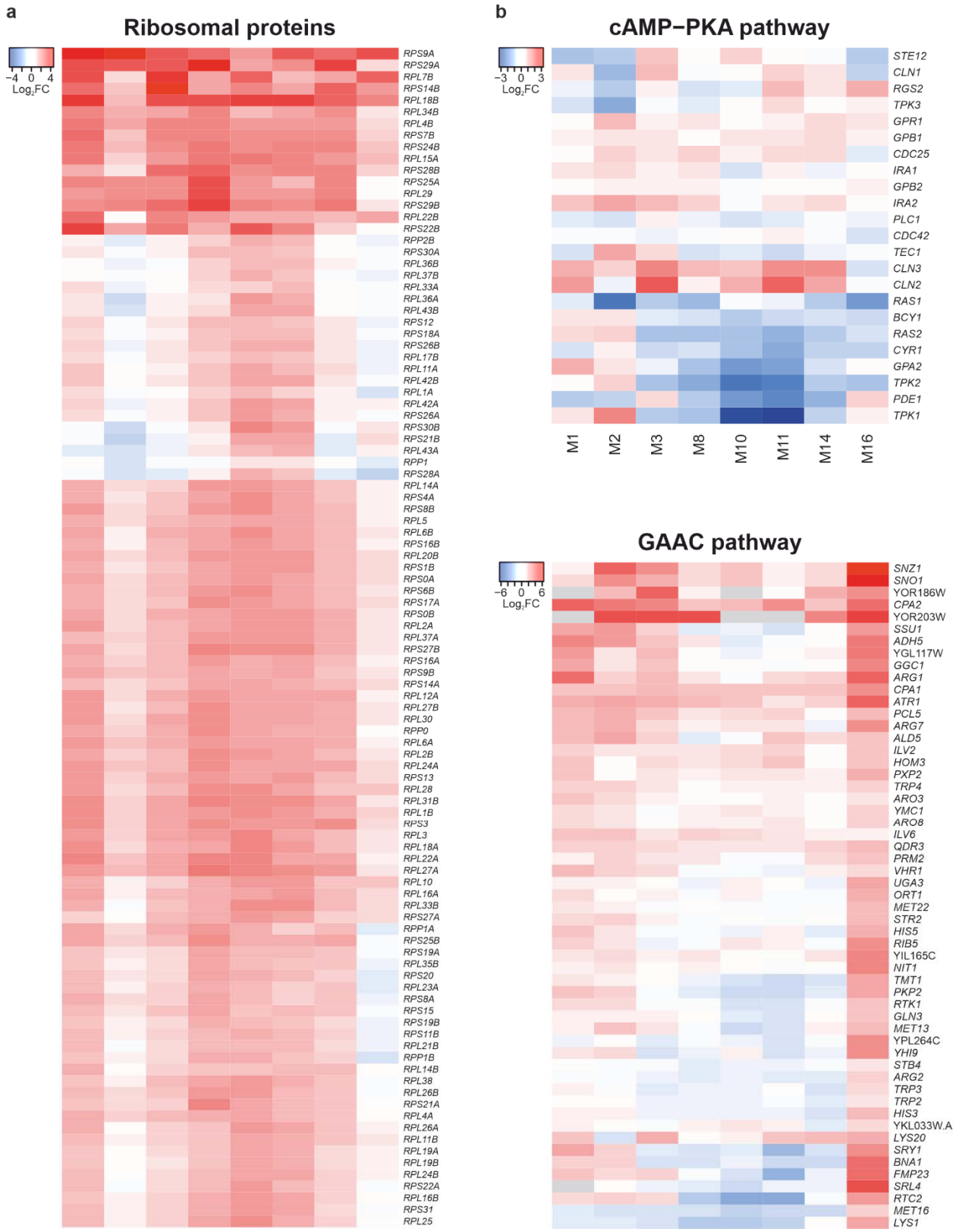
a
Ribosomal proteins
−4 0 4
Log2FC
RPS9A
RPS29A
RPL7B
RPS14B
RPL18B
RPL34B
RPL4B
RPS7B
RPS24B
RPL15A
RPS28B
RPS25A
RPL29
RPS29B
RPL22B
RPS22B
RPP2B
RPS30A
RPL36B
RPL37B
RPL33A
RPL36A
RPL43B
RPS12
RPS18A
RPS26B
RPL17B
RPL11A
RPL42B
RPL1A
RPL42A
RPS26A
RPS30B
RPS21B
RPL43A
RPP1
RPS28A
RPL14A
RPS4A
RPS8B
RPL5
RPL6B
RPS16B
RPL20B
RPS1B
RPS0A
RPS6B
RPS17A
RPS0B
RPL2A
RPL37A
RPS27B
RPS16A
RPS9B
RPS14A
RPL12A
RPL27B
RPL30
RPP0
RPL6A
RPL2B
RPL24A
RPS13
RPL28
RPL31B
RPL1B
RPS3
RPL3
RPL18A
RPL22A
RPL27A
RPL10
RPL16A
RPL33B
RPS27A
RPP1A
RPS25B
RPS19A
RPL35B
RPS20
RPL23A
RPS8A
RPS15
RPS19B
RPS11B
RPL21B
RPP1B
RPL14B
RPL38
RPL26B
RPS21A
RPL4A
RPL26A
RPL11B
RPL19A
RPL19B
RPL24B
RPS22A
RPL16B
RPS31
RPL25
b
cAMP−PKA pathway
−3 0 3
Log2FC
STE12
CLN1
RGS2
TPK3
GPR1
GPB1
CDC25
IRA1
GPB2
IRA2
PLC1
CDC42
TEC1
CLN3
CLN2
RAS1
BCY1
RAS2
CYR1
GPA2
TPK2
PDE1
TPK1
M1
M2
M3
M8
M10
M11
M14
M16
GAAC pathway
−6 0 6
Log2FC
SNZ1
SNO1
YOR186W
CPA2
YOR203W
SSU1
ADH5
YGL117W
GGC1
ARG1
CPA1
ATR1
PCL5
ARG7
ALD5
ILV2
HOM3
PXP2
TRP4
ARO3
YMC1
ARO8
ILV6
QDR3
PRM2
VHR1
UGA3
ORT1
MET22
STR2
HIS5
RIB5
YIL165C
NIT1
TMT1
PKP2
RTK1
GLN3
MET13
YPL264C
YHI9
STB4
ARG2
TRP3
TRP2
HIS3
YKL033W.A
LYS20
SRY1
BNA1
FMP23
SRL4
RTC2
MET16
LYS1

785

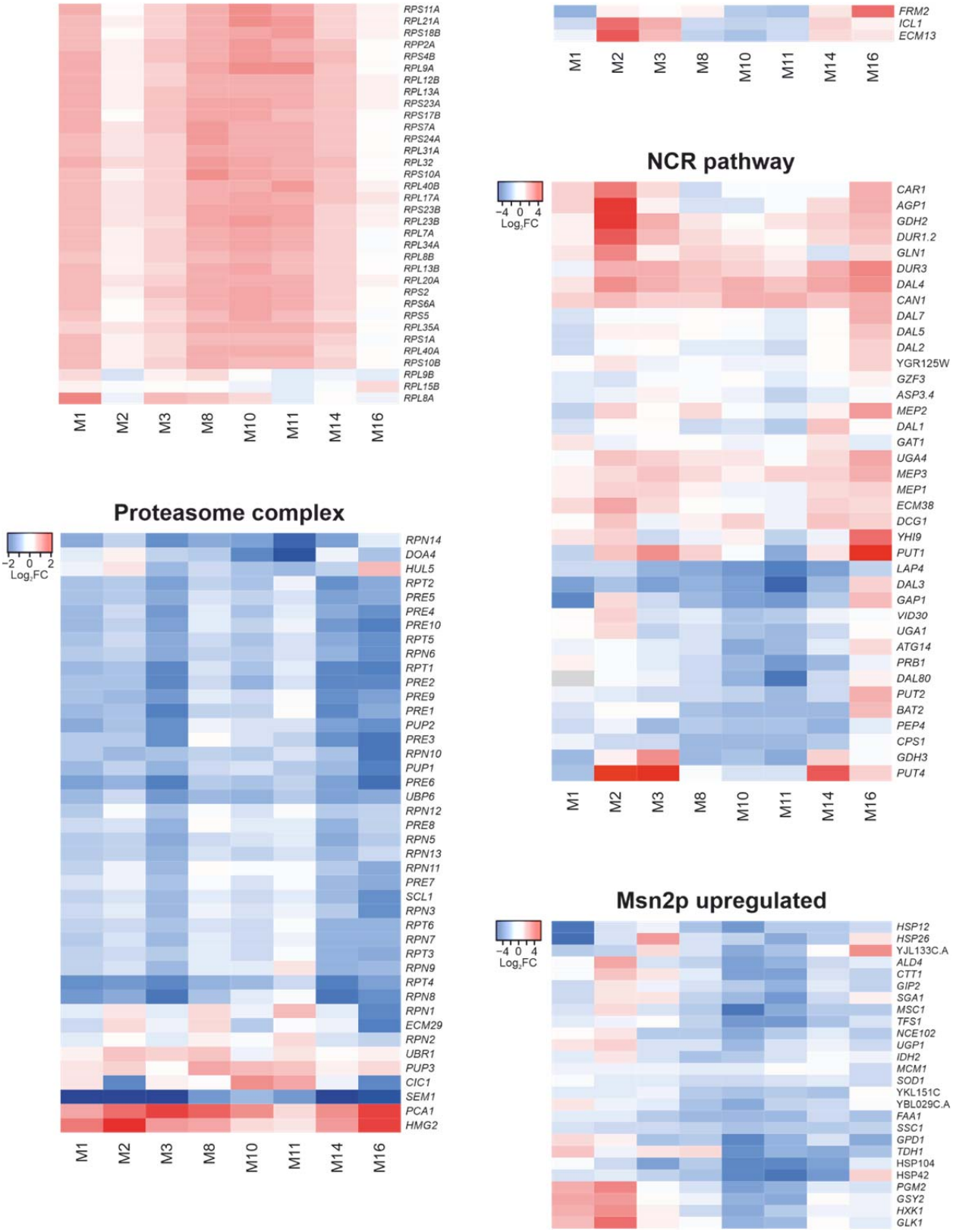
RPS11A
RPL21A
RPS18B
RPP2A
RPS4B
RPL9A
RPL12B
RPL13A
RPS23A
RPS17B
RPS7A
RPS24A
RPL31A
RPL32
RPS10A
RPL40B
RPL17A
RPS23B
RPL23B
RPL7A
RPL34A
RPL8B
RPL13B
RPL20A
RPS2
RPS6A
RPS5
RPL35A
RPS1A
RPL40A
RPS10B
RPL9B
RPL15B
RPL8A
M1 M2 M3 M8 M10 M11 M14 M16
FRM2
ICL1
ECM13
M1 M2 M3 M8 M10 M11 M14 M16
NCR pathway
−4 0 4
Log2FC
CAR1
AGP1
GDH2
DUR1.2
GLN1
DUR3
DAL4
CAN1
DAL7
DAL5
DAL2
YGR125W
GZF3
ASP3.4
MEP2
DAL1
GAT1
UGA4
MEP3
MEP1
ECM38
DCG1
YHI9
PUT1
LAP4
DAL3
GAP1
VID30
UGA1
ATG14
PRB1
DAL80
PUT2
BAT2
PEP4
CPS1
GDH3
PUT4
M1 M2 M3 M8 M10 M11 M14 M16
Proteasome complex
−2 0 2
Log2FC
RPN14
DOA4
HUL5
RPT2
PRE5
PRE4
PRE10
RPT5
RPN6
RPT1
PRE2
PRE9
PRE1
PUP2
PRE3
RPN10
PUP1
PRE6
UBP6
RPN12
PRE8
RPN5
RPN13
RPN11
PRE7
SCL1
RPN3
RPT6
RPN7
RPT3
RPN9
RPT4
RPN8
RPN1
ECM29
RPN2
UBR1
PUP3
CIC1
SEM1
PCA1
HMG2
M1 M2 M3 M8 M10 M11 M14 M16
Msn2p upregulated
−4 0 4
Log2FC
HSP12
HSP26
YJL133C.A
ALD4
CTT1
GIP2
SGA1
MSC1
TFS1
NCE102
UGP1
IDH2
MCM1
SOD1
YKL151C
YBL029C.A
FAA1
SSC1
GPD1
TDH1
HSP104
HSP42
PGM2
GSY2
HXK1
GLK1

786

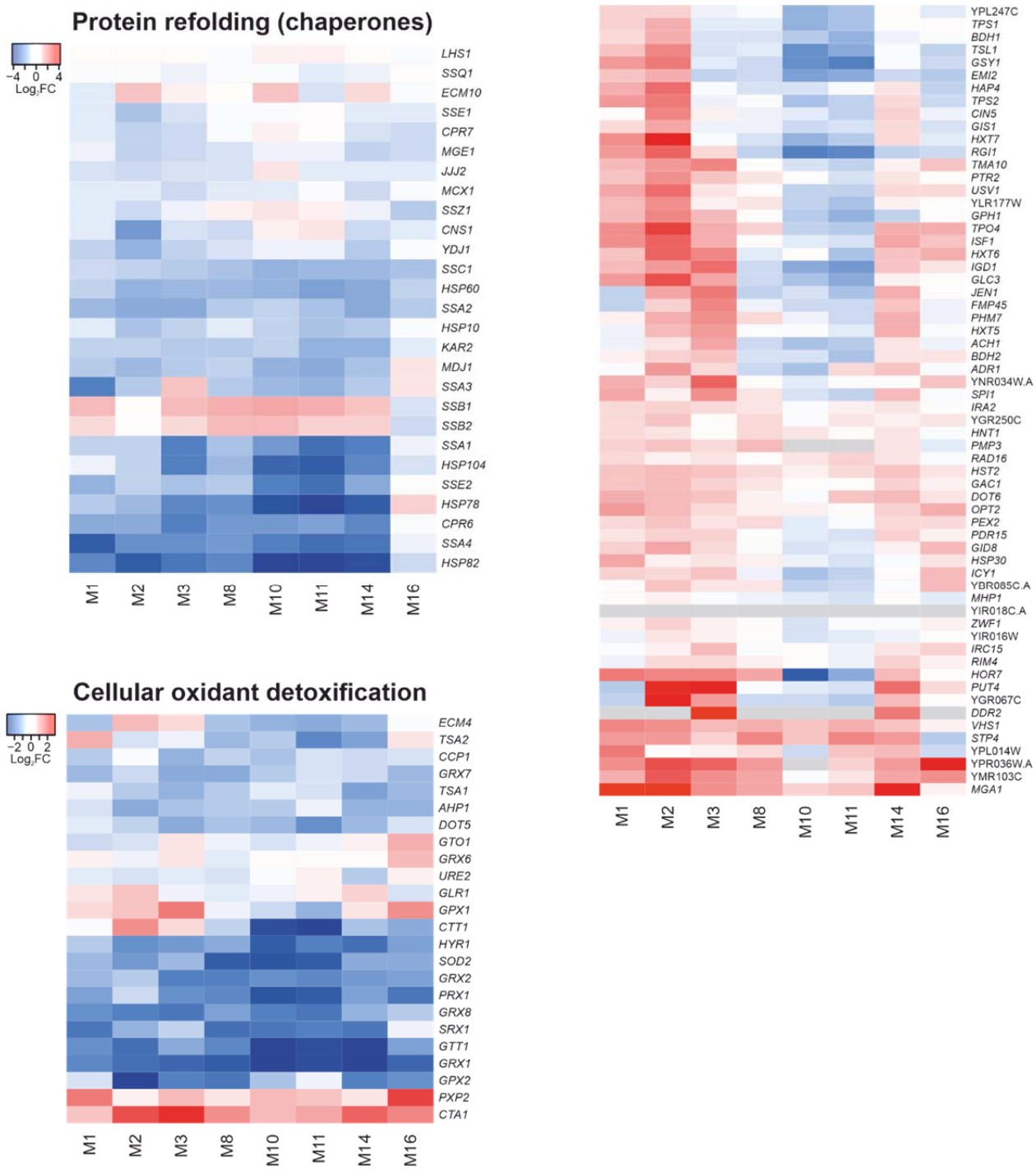

Supplementary Figure S1. Parallel and divergent shifts in transcriptomes of monosomic strains. Heat maps show monosomic mRNA frequencies divided by respective diploid (control) ones. (**a**) Gene Ontology categories selected to demonstrate similarities in transcriptional profiles of monosomic strains. (**b**) Regulons demonstrating differences in gene expression between monosomic strains. (This figure is an expanded version of Fig. 4 in the main text.)

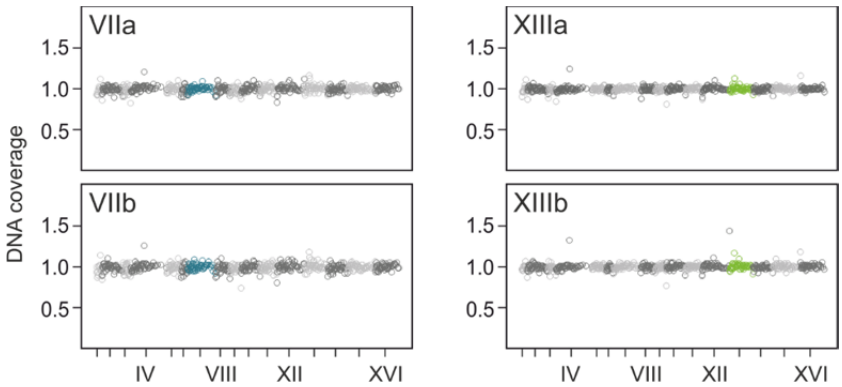

Supplementary Figure S2. DNA whole genome sequencing coverage after the postulated endoreduplication. Two isolates descending from the parental diploid strains with marked chromosomes VII or XIII are shown. They were subjected to sequencing after being found to lack phenotypic markers and produce four viable spores.